Bimodal Intramolecular Excitation Energy Transfer in a Multichromophore Photosynthetic Model System: Hybrid Fusion Proteins Comprising Natural Phycobilin- and Artificial Chlorophyl...

ARTICLE *in* JOURNAL OF THE AMERICAN CHEMICAL SOCIETY · AUGUST 2013

Impact Factor: 12.11 · DOI: 10.1021/ja405617c · Source: PubMed

JACS
JOURNAL OF THE AMERICAN CHEMICAL SOCIETY

Article

pubs.acs.org/JACS

Bimodal Intramolecular Excitation Energy Transfer in a Multichromophore Photosynthetic Model System: Hybrid Fusion Proteins Comprising Natural Phycobilin- and Artificial Chlorophyll-Binding Domains

Xiao-Li Zeng,[†] Kun Tang,[†] Nan Zhou,[†] Ming Zhou,[†] Harvey J. M. Hou,[‡] Hugo Scheer,[§] Kai-Hong Zhao,[†,*] and Dror Noy[#,∥,⊥]

[†]State Key Laboratory of Agricultural Microbiology, Huazhong Agricultural University, Wuhan 430070, P.R. China

[‡]Department of Physical Sciences, Alabama State University, 915 South Jackson Street, Montgomery, Alabama 36104, United States

[§]Department Biologie I, Universität München, Menzinger Str. 67, D-80638 München, Germany

[∥]Plant Sciences Department, Weizmann Institute, Rehovot 7610001, Israel

[⊥]Migal – Galilee Research Institute, South Industrial Zone, Kiryat Shmona 1101602, Israel

Supporting Information

ABSTRACT: The phycobilisomes of cyanobacteria and red-algae are highly efficient peripheral light-harvesting complexes that capture and transfer light energy in a cascade of excitation energy transfer steps through multiple phycobilin chromophores to the chlorophylls of core photosystems. In this work, we focus on the last step of this process by constructing simple functional analogs of natural phycobilisome–photosystem complexes that are based on bichromophoric protein complexes comprising a phycobilin- and a chlorophyll- or porphyrin-binding domain. The former is based on ApcE(1–240), the N-terminal chromophore-binding domain of the phycobilisome's L_{CM} core-membrane linker, and the latter on HP7, a *de novo* designed four-helix bundle protein that was originally planned as a high-affinity heme-binding protein, analogous to *b*-type cytochromes. We fused a modified HP7 protein sequence to ApcEΔ, a water-soluble fragment of ApcE(1–240) obtained by excising a putative hydrophobic loop sequence of residues 77–153. HP7 was fused either to the N- or the C-terminus of ApcEΔ or inserted between residues 76 and 78, thereby replacing the native hydrophobic loop domain. We describe the assembly, spectral characteristics, and intramolecular excitation energy transfer of two unique systems: in the first, the short-wavelength absorbing zinc-mesoporphyrin is bound to the HP7 domain and serves as an excitation-energy donor to the long-wavelength absorbing phycocyanobilin bound to the ApcE domain; in the second, the short-wavelength absorbing phycoerythrobilin is bound to the ApcE domain and serves as an excitation energy donor to the long-wavelength absorbing zinc-bacteriochlorophyllide bound to the HP7 domain. All the systems that were constructed and tested exhibited significant intramolecular fluorescence resonance energy transfer with yields ranging from 21% to 50%. This confirms that our modular, covalent approach for studying EET between the cyclic and open chain tetrapyrroles is reasonable, and may be extended to larger structures mimicking light-harvesting in cyanobacteria. The design, construction, and characterization process demonstrated many of the advances in constructing such model systems, particularly in our ability to control the fold and aggregation state of protein-based systems. At the same time, it underlines the potential of exploiting the versatility and flexibility of protein-based systems in assembling multiple pigments into effective light-harvesting arrays and tuning the spectral properties of multichromophore systems.

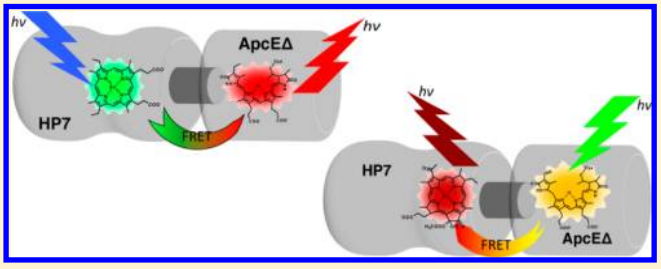

INTRODUCTION

The effective capture of incoming light is critical to the efficiency of solar energy conversion systems.[1] Natural selection of photosynthetic organisms has brought about the modular photosystem architecture as an elegant solution to the problem. All photosynthetic organisms employ transmembranal pigment–protein complexes comprising chlorophylls (Chls) or bacteriochlorophylls (BChls) as their core light-harvesting complexes (LHCs). The majority of pigments are contained in a variety of taxon-specific peripheral LHCs. Cyanobacteria and red algae, which account for a substantial fraction of global photosynthesis, evolved the phycobilisome (PBS) as a highly sophisticated and dynamic peripheral LHC.[2] These water-soluble extra-membranous multiprotein complexes may reach a molecular weight of several millions and bind hundreds of

Received: June 5, 2013
Published: August 13, 2013

   dx.doi.org/10.1021/ja405617c | J. Am. Chem. Soc. 2013, 135, 13479–13487

phycobilin chromophores by covalent attachment to cysteines at specific protein binding sites. The large number of possible combinations of phycobilin derivatives and protein subunits enable cyanobacteria to adapt their light absorption to the different light environments encountered in aquatic ecosystems.

A hallmark of PBS activity is the highly efficient transfer of captured light energy to the photosynthetic core complexes in a cascade of excitation energy transfer (EET) steps from the blue-green absorbing phycoerythrin (or phycoerythrocyanin in some heterocystous cyanobacteria) and the orange absorbing phycocyanin via the red absorbing allophycocyanin and, eventually, the core-membrane linker, L_{CM}, to the Chls of (mainly) photosystem II (PSII). In this work, we focus on the last step by constructing simple functional analogs of natural PBS-photosystem complexes that are based on bichromophoric protein complexes comprising a phycobilin- and a Chl- or porphyrin-binding domain. The phycobilin-binding domain is based on ApcE(1−240), the N-terminal chromophore-binding domain of the L_{CM} core-membrane linker.[3] Native L_{CM} is encoded by the *apcE* gene; the product, ApcE, is a large, multidomain protein of 75 to 125 kDa that autocatalytically binds a phycocyanobilin (PCB) chromophore. The chromophore is covalently bound to a cysteine residue near the N-terminus of the phycobiliprotein. ApcE(1−240) is still only poorly water-soluble; it contains a putative hydrophobic loop between residues 80 and 150, which may anchor the PBSs to the thylakoid membrane. Removal of residues 77−153 resulted in a water-soluble fragment ApcE(1−240/Δ77−153), ApcEΔ, that retains ApcE's unique capability of autocatalytic covalent attachment of free phycobilin chromophores, both in vivo[4,5] and in vitro.[3] The chlorophyll-binding domain is based on HP7, a *de novo* designed four-helix bundle protein. HP7 was originally prepared as a high-affinity heme-binding protein, analogous to *b*-type cytochromes.[6] The water-soluble, 62-residues protein has a helix−loop−helix topology with a histidine residue on each helix. These form two bis-histidine heme-binding sites upon the spontaneous assembly of the protein into a four-helix bundle dimer.[7] HP7 can incorporate other metalloporphyrin derivatives in its heme-binding sites. Recently, the assembly of HP7 with the water-soluble zinc-substituted bacteriochlorophyllide-*a* derivative, 13^2-OH-[Zn]-bacteriochlorophyllide-*a* (ZnBC), was rigorously characterized by one of us.[8]

In this work, a modified HP7 sequence was fused either to the N- or the C-terminus of ApcEΔ, or inserted between residues 76 and 78, thereby replacing the putative loop domain at residues 77 to 153 of the native ApcE sequence.[9] The new fusion proteins labeled HP7::ApcEΔ, ApcEΔ::HP7, and $ApcE\Delta_N$::HP7::$ApcE\Delta_C$, respectively, are potential bichromophoric systems that combine one binding site for phycobilin derivatives with another for porphyrin, chlorin, or bacteriochlorin derivatives (Figure 1). We describe the assembly, spectral characteristics, and intramolecular EET of two unique systems: in the first, the short-wavelength absorbing porphyrin, ZnMP, is bound to the HP7 domain and serves as an excitation energy donor to the long-wavelength absorbing phycobilin, PCB, bound to the ApcE domain; in the second, the short-wavelength absorbing phycobilin, PEB, is bound to the ApcE domain and serves as an excitation energy donor to the long-wavelength absorbing bacteriochlorin, ZnBC, bound to HP7 domain.

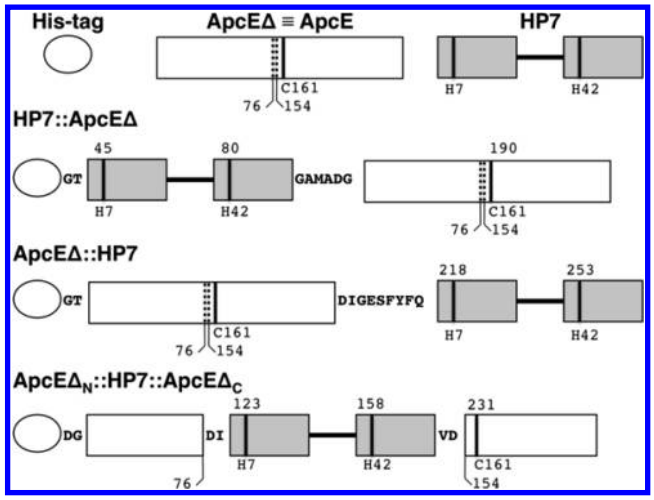

Figure 1. Domain architecture of three fusion proteins combining the ApcEΔ fragment of the natural L_{CM} PBS membrane linker, and HP7, a *de novo* designed heme and chlorophyll binding protein. The position of the truncated putative membrane anchor of ApcE is marked by two dotted lines. The positions of the heme binding histidines of HP7 (H7 and H42) and of the phycobilin binding cysteine (C161) of ApcE are marked by solid lines. Their actual positions in each new fusion protein sequence are marked above each line.

RESULTS

Autocatalytic Chromophorylation of the ApcE Domain. All fusion proteins shown in Figure 1 were expressed as soluble proteins in *E. coli*, and were autocatalytically chromophorylated with PCB or PEB in low yields (Table 1). Chromatographic separation of the crude protein−pigment complexes significantly enriched the samples in the chromophorylated proteins, with the exception of PEB-chromophorylated $ApcE\Delta_N$::HP7::$ApcE\Delta_C$ (Table 1, Figure 2). In most fusion proteins, chromophorylation was significantly improved, both in the crude fractions and in the purified samples. The characteristic absorption of PEB-chromophorylated fusion proteins was the same as PEB-chromophorylated ApcEΔ (Figure 2). By contrast, the characteristic absorption of PCB was blue-shifted in the fusion proteins compared with chromophorylated ApcEΔ. This shift was small (4 nm) in chromophorylated HP7::ApcEΔ, and ApcEΔ::HP7, but larger (22 nm) in chromophorylated $ApcE\Delta_N$::HP7::$ApcE\Delta_C$. The fluorescence emission bands of both PCB and PEB in the chromophorylated fusion proteins were the same as in chromophorylated ApcEΔ, except for the PCB chromophorylated $ApcE\Delta_N$::HP7::$ApcE\Delta_C$ that showed a 8 nm blue shift (Figure 2). The absorption of the open-chain bilin chromophores in biliproteins is largely determined by non-covalent pigment−protein interactions. In particular, the absorption of PCB is strongly red-shifted in ApcE. The retention of most of this large red-shift in HP7::ApcEΔ, and ApcEΔ::HP7 is indicative of only a little change in the bilin binding pocket. The blue shift in $ApcE\Delta_N$::HP7::$ApcE\Delta_C$ indicates a more significant change, but even in this case part of the ApcE-characteristic red-shift is retained.

Binding of Heme, ZnMP, or ZnBC to the HP7 Domain. The integrity and functionality of the HP7 domain in the fusion proteins was first evaluated by the heme binding capacity. Since HP7 has two histidines that comprise only half of each binding site, it is incapable of heme binding as a monomer; however, it spontaneously forms homodimers that assemble into four helix-

Table 1. Extinction Coefficients and PCB/PEB Chromophorylation Yields for HP7-ApcEΔ Fusion Proteins

		ApcEΔ	HP7::ApcEΔ	$ApcEΔ_N$::HP7::$ApcEΔ_C$	ApcEΔ::HP7
Apo	ε_{prot} (mM^{-1} cm^{-1})	13	24	24	25
PCB	yield (enriched[a]/crude)	70/4.5%	95/26%	75/9.4%	98/19%
	ε_{UV} [mM^{-1} cm^{-1}]	21	23	21	16
	ε_{VIS} [mM^{-1} cm^{-1}] (λ[nm])	91 (661)	94 (657)	74 (639)	74 (657)
PEB	yield (enriched[a]/crude)	47/14%	58/9.4%	9/8%	91/17%
	ε_{UV} [mM^{-1} cm^{-1}]	38	30	24	12
	ε_{VIS} [mM^{-1} cm^{-1}] (λ[nm])	91 (578)	94 (578)	82 (578)	90 (578)

[a]After chromatographic purification.

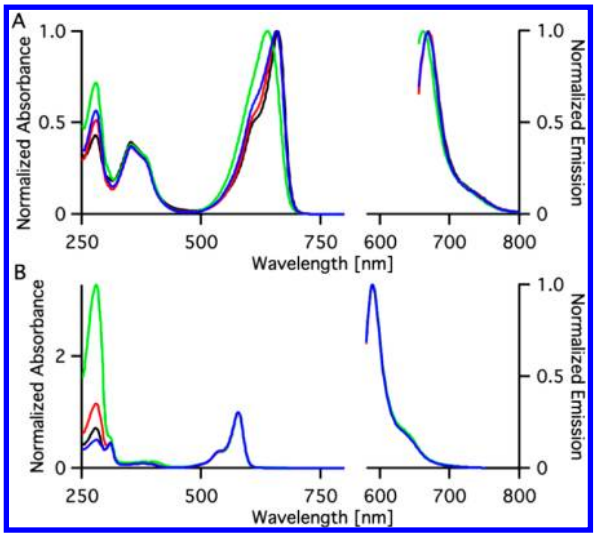

Figure 2. Absorption (left) and emission (right) spectra of PCB- (A) and PEB- (B) chromophorylated ApcEΔ (black), HP7::ApcEΔ (red), ApcEΔ::HP7 (blue), $ApcEΔ_N$::HP7::$ApcEΔ_C$ (green). Spectra were normalized at the peak of the visible absorption or emission bands.

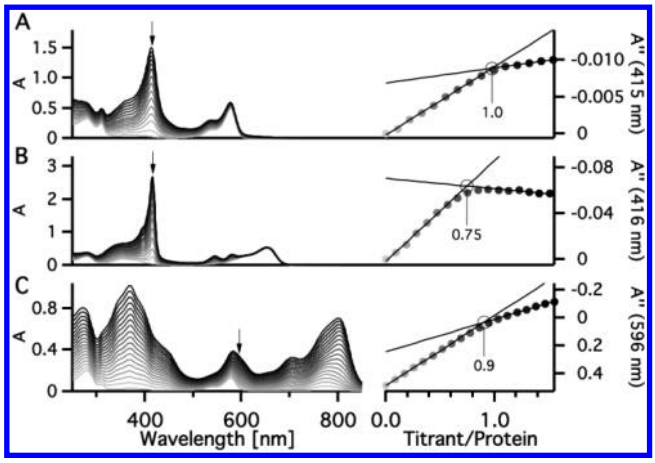

Figure 3. Titrations and saturation binding curves of PEB-chromophorylated ApcEΔ::HP7 titrated with heme (A), PCB-chromophorylated HP7::ApcEΔ titrated with ZnMP (B), and PEB-chromophorylated HP7::ApcEΔ titrated with ZnBC (C). For better resolution, the binding curves were constructed from the second derivative value at 596, 416, and 415 nm, corresponding to the respective peak absorption of bound ZnBC, ZnMP, and heme. These wavelengths are marked by arrows on the respective absorption spectra.

bundles with two bis-histidine heme-binding sites.[6] The maximal binding capacity is two hemes per such a dimer, resulting in a stoichiometry of one heme per HP7. Originally, a cysteine was placed in the middle of the loop connecting HP7's two helices. Its role was to form a disulfide bond between two HP7 monomers that would lock the homodimer in a *syn* four-helix bundle topology.[7,17] We relieved this restriction by replacing this cysteine with a serine to allow more conformational flexibility in the HP7-ApcEΔ fusion proteins. Chromophorylated and non-chromophorylated fusion proteins were titrated with heme to determine their binding capacity. Titration of 13 μM PEB-chromophorylated ApcEΔ::HP7 is shown in Figure 3A. The characteristic heme absorption peak at 413 nm is the most apparent marker for heme binding by the protein. The peak intensity increases linearly with heme concentration until the protein binding capacity is exceeded, which is indicative of complete binding. Beyond the saturation point, the heme absorption band is blue-shifted due to the emergence of an absorption peak of unbound heme at 399 nm. Thus, plotting the 413 nm peak intensity as a function of heme/protein ratio yielded a saturation binding curve from which the heme binding stoichiometries were determined (Figure 3A, Table 2). The heme binding capacity for all fusion proteins was found to be close to the expected one heme per HP7; that is, two per dimer, irrespective of the presence or absence of a phycobilin chromophore in the ApcEΔ domain, or of the type of phycobilin chromophore bound (Table 2). This is supported by size exclusion chromatography analysis (see below). It suggests that the ApcE domain does not prevent the assembly of HP7 dimers into four-helix bundles, which is required for heme binding. Interestingly, this occurs irrespective of the position of the HP7 domain. Apparently, dimerization of the HP7 domains is a dominant protein−protein interaction in all constructs.

Unfortunately, heme is unsuitable for resonance EET to or from phycobilin derivatives because it is nonfluorescent, and its main absorption band is too far to the blue from any phycobilin emission band for resonance EET. Since helical bundles similar to HP7 have been shown to bind fluorescent zinc-porphyrin derivatives,[18,19] we chose to incorporate ZnMP into the HP7 domain of our fusion proteins. ZnMP is a suitable excitation energy donor to PCB because its significant fluorescence emission band at 630 nm overlaps the lowest energy absorption band of PCB. We determined the ZnMP binding capacity of PCB-chromophorylated proteins and their respective apoproteins by the same method as described for heme binding. Figure 3B shows the titration of 11.5 μM PCB-chromophorylated HP7::ApcEΔ with ZnMP. Here, the Soret absorption of bound ZnMP peaks at 416 nm, which is a red shift of 12 nm with respect to ZnMP in protein free buffer. In contrast to heme, analysis of the saturation binding curves of ZnMP yielded different binding capacities for each fusion protein which, furthermore, varied between chromophorylated and non-chromophorylated proteins. Yet, all values were between

dx.doi.org/10.1021/ja405617c | J. Am. Chem. Soc. 2013, 135, 13479−13487

Table 2. Titration of Heme, ZnMP, ZnBC into the HP7 Domain of Various HP7-ApcE Fusion Proteins, and Aggregation States of the Constructs Determined by Gel Filtration

pigment bound to HP7		pigment/HP7 molar ratio (N_{agg})[a]			
fusion protein	phycobilin	none	heme	ZnMP	ZnBC
HP7::ApcEΔ	None	−(2.6)	0.97 (2.6)	0.73 (2.6)	1.1 (2.6, 5.9; 3:2)
	PCB	−(1.8)	0.85 (2.5)	0.75 (1.8, 2.6; 2:1)	n.d.[b]
	PEB	−(1.7)	0.95 (2.6)	n.d.[b]	0.9 (1.7, 2.5, 5.7; 1:5:2)
ApcEΔ$_N$::HP7::ApcEΔ$_C$	None	−(8.8)	0.95 (6.1, 9.1; 5:4)	0.75 (8.9)	0.86 (8.8)
	PCB	−(3.3, 8.6; 1:4)	0.9 (6)	0.5 (2.9,8.8; 2:3)	n.d.[b]
	PEB	−(2.0, 8.8; 1:2)	1.0 (8.9)	n.d.[b]	1.0 (5.8, 8.8; 2:3)
ApcEΔ::HP7	None	−(3.1)	0.94 (2.5, 5.5; 2:3)	0.6 (2.6)	0.75 (2.4, 5.1 2:1)
	PCB	−(2.5)	1.2 (2.5, 5.4, 8.5; 3:4:3)	0.67 (2.4)	n.d.[b]
	PEB	−(2.8)	1.0 (2.8, 4.9; 1:1)	n.d.[b]	1.0 (2.4)

[a]Aggregation numbers, N_{agg}, were calculated by dividing the apparent molecular weight by the calculated apoprotein monomer's molecular weight of 23.6, 30.1, 30.4, and 31.2 kDa for ApcEΔ, HP7::ApcEΔ, ApcEΔN::HP7::ApcEΔ$_C$, and ApcEΔ::HP7, respectively. In the case of multiple bands, the relative peak intensities are indicated after the semicolon. The aggregation numbers of non-, PCB-, and PEB-chromophorylated ApcEΔ were found to be 2.0, 2.6, and 3, respectively. [b]Not determined.

0.5 and 0.85 pigments per protein monomer, suggesting that all proteins have at least one high-affinity binding site available for ZnMP in their HP7 domain.

The binding of ZnBC to HP7 has been thoroughly characterized.[8] HP7 is capable of binding up to three ZnBC per four-helix bundle dimer. Upon binding, histidine coordination red-shifts the Q_x absorption band of ZnBC to 590 nm, which makes it a potential acceptor of excitation energy from PEB. The ZnBC binding capacities of PEB-chromophorylated and nonchromophorylated fusion proteins were also determined by titration, as shown in Figure 3C for PEB-chromophorylated HP7::ApcEΔ. The emergence of a characteristic ZnBC absorption band at 590 nm is clearly visible adjacent to the PEB absorption peak at 578 nm. The emerging absorption peak at 776 nm is also typical of the Q_y band of HP7-bound ZnBC. This band is further red-shifted to 805 nm with the increase of ZnBC concentration, which indicates the formation of an excitonically coupled ZnBC dimer.[8] The ZnBC binding capacities of all fused apoproteins and PEB chromophorylated proteins were found to be similar to the heme binding capacities; that is, one ZnBC pigment per monomer (Table 2). However, the formation of excitonically coupled ZnBC dimers is indicative of binding two ZnBC pigments in a single heme-binding site.[8] Titrations of ApcEΔ with heme, ZnMP, or, ZnBC (not shown) did not result in the typical red-shifted absorption bands that were observed for HP7-bound pigments. The linear dependence of peak intensity on pigment concentration indicated that, as expected, there is no specific binding of these cyclic tetrapyrroles to the ApcE domain.

Aggregation States of ApcEΔ and Fusion Proteins. Phycobiliproteins tend to form homo- and hetero-oligomers as part of their self-assembly into the various functional units of PBSs. Water-soluble ApcE fragments form homodimers in solution.[5] We have demonstrated above the binding of pigments to the HP7 domain of the fusion proteins, which requires its self-assembly into a homodimeric four-helix bundle. Therefore, it is very likely that the new HP7-ApcEΔ fusion proteins form oligomers in solution. Analytical size exclusion chromatography revealed complex aggregation of ApcEΔ and its fusion protein that depend on protein type, chromophorylation of the ApcE domain, and pigment binding to the HP7 domain (Table 2). Yet, there was no evidence for monomers in any of the samples: the nominal aggregation state, N_{agg}, appeared, in most cases, to be dimer and/or trimer. Size exclusion chromatography measures the hydrodynamic size rather than the actual molecular weight of the proteins and their pigment complexes; thus, the observed range of nominal aggregation numbers, N_{agg} = 1.7−3.3, may still be attributed to protein dimers of different shapes. The only exception is the ApcEΔ$_N$::HP7::ApcEΔ$_C$ fusion that appeared to form higher aggregates, formally nonamers. Interestingly, N_{agg} of HP7::ApcEΔ and ApcEΔ::HP7 decreased upon chromophorylation, indicating a more compact shape, while ApcEΔ appeared to be more compact as apoprotein.

Irrespective of oligomerization, the fluorescence anisotropy spectra of fusion proteins singly chromophorylated with PCB or PEB indicated that the bound phycobilins were not interacting (Supporting Information (SI) Figure S1). With no exception, the spectra of all PCB- and PEB-ApcE complexes featured anisotropy values in the long-wavelength region that were close to the theoretical maximum of 0.4. The values for the lowest energy excited state range from 0.29 to 0.37; they are similar to those found in allophycocyanin monomers that carry a single chromophore.[20] While we cannot exclude a parallel orientation of the chromophores in oligomers, it is reasonable to assume from these data that protein oligomerization does not bring the bound phycobilin chromophores within resonance EET distances.

Intramolecular Excitation Energy Transfer in Bichromophoric Fusion Proteins. After establishing the binding stoichiometry of ZnMP and ZnBC to HP7-ApcEΔ fusion proteins we selected two donor−acceptor systems for investigating resonance EET; namely, a ZnMP-PCB and a PEB-ZnBC system. In the first system HP7-bound ZnMP acts as donor: when excited at its 415 nm absorption peak, ZnMP has two fluorescence emission bands at 583 and 628 nm of which the latter band significantly overlaps with the absorption band of ApcE-bound PCB (Figure 4B), which then emits at 666 nm. In the second system, ApcE-bound PEB acts as donor: when excited at 570 nm, it emits at 587 nm (Figure 4A), which overlaps very well with the Q_x absorption band of HP7-bound ZnBC. Relaxation to the lowest excited state then results in emission in the near-infrared at 787 nm. Both systems show very large Stokes shifts. Back energy transfer from acceptors to donors is expected to be negligible in both systems because the donors have almost no absorption in the wavelength range of the acceptors' emission bands.

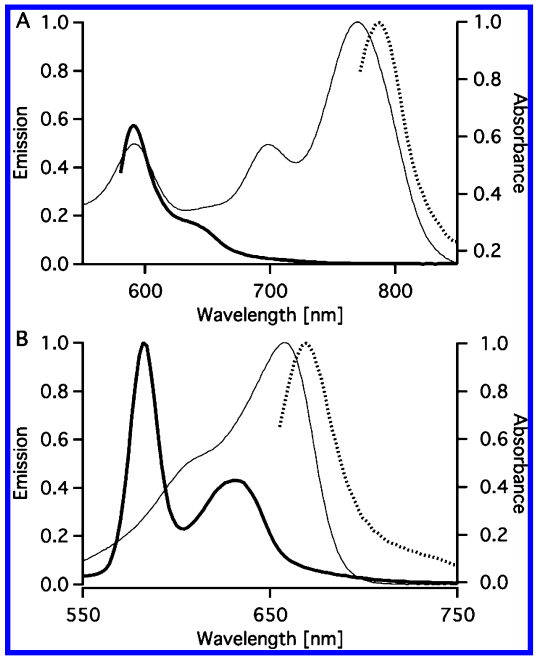

Figure 4. Donor emission (thick solid line), and acceptor absorbance (thin line) and emission (dotted line) spectra of the PEB→ZnBC (A) and ZnMP→PCB (B) donor–acceptor systems.

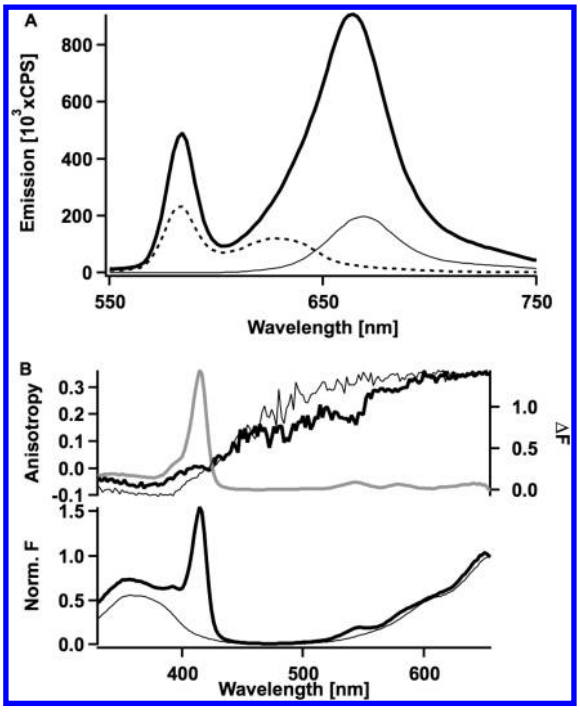

Figure 5. Fluorescence emission (A, λ_{ex} = 415 nm), excitation and anisotropy spectra (B, λ_{em} = 675 nm) of the bichromophorylated ZnMP→PCB systems in HP7::ApcEΔ. (A) PCB-chromophorylated (thin line), and ZnMP in PCB-chromophorylated and non-chromophorylated (thick dotted and solid lines, respectively) (B) Top: PCB anisotropy spectra of proteins with or without ZnMP (thin and thick black lines, respectively) and difference between their normalized excitation spectra (grey line). Bottom: PCB excitation spectra of proteins with or without ZnMP (thin and thick lines, respectively) normalized at 654 nm (640 nm, for ApcEΔ$_N$::HP7::ApcEΔ$_C$).

Characteristic emission, excitation, and anisotropy spectra of the ZnMP→PCB system indicating significant EET from ZnMP to PCB in the bichromophoric systems are shown in Figure 5. In all bichromophoric complexes, excitation at 415 nm into the ZnMP absorption maximum led to enhanced PCB emission. The fluorescence excitation spectra, recorded at a PCB-specific emission wavelength of 675 nm, show strong ZnMP excitation bands in the bichromophoric systems and the difference between PCB-ZnMP and PCB excitation spectra correspond to the absorption spectra of ZnMP. Furthermore, the fluorescence anisotropy of the 675 nm emission is significantly decreased in the region of the ZnMP Q-absorption band, as expected for EET among nonparallel transitions. Titration of PCB-chromophorylated fusion proteins with ZnMP yielded the expected saturation binding-curve when plotting the PCB normalized fluorescence as a function of ZnMP concentration (Figure 6). The EET yields calculated from the linear region of each plot prior to saturation range between 20% and 50% (Table 3; see Experimental Section for details).

The results for the PEB→ZnBC system are shown in Figure 7. The control is ZnBC in nonchromophorylated fusion proteins. The emission of ZnBC at 790 nm in PEB-ZnBC bichromophorylated HP7::ApcEΔ and ApcEΔ::HP7 complexes is enhanced, and the fluorescence emission of PEB at 587 nm is decreased with respect to the same proteins chromophorylated only with ZnBC or PEB, respectively. It is difficult to determine how much of the decrease in PEB emission is attributed to resonance EET and how much is due to conformational changes due to the binding of ZnBC to the HP7 domain; however, the enhanced ZnBC fluorescence at 790 nm and the difference excitation spectra of this emission band that correspond to PEB absorption spectra (Figure 7B) are clear indications of significant EET from PEB to ZnBC. Indeed, the calculated EET yields (Table 3) are similar to the respective yields of the ZnMP-PCB donor–acceptor system.

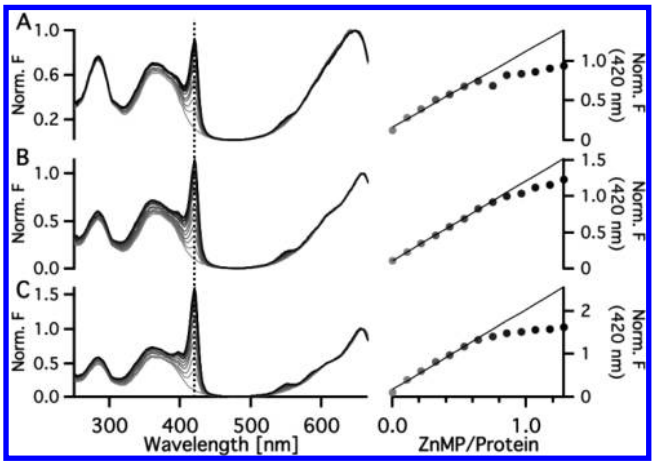

Figure 6. Left: Fluorescence excitation spectra of the bichromophorylated ZnMP→PCB systems ApcEΔ$_N$::HP7::ApcEΔ$_C$ (A), ApcEΔ::HP7 (B), and HP7::ApcEΔ (C) titrated with ZnMP. Emission is detected at 675 nm and the spectra are normalized at the red-most excitation peak of PCB (646 nm for HP7::ApcEΔ::HP7, and 658 nm for ApcEΔ::HP7 and HP7::ApcEΔ). The dashed line marks the excitation band at 420 nm that is due to EET for ZnMP to PCB. Right: Saturation binding curves were constructed by plotting the band's intensity as a function of ZnMP to protein molar ratios.

ApcEΔ$_N$::HP7::ApcEΔ$_C$ complexes were not tested because of their low PEB chromophorylation yields.

dx.doi.org/10.1021/ja405617c | J. Am. Chem. Soc. 2013, 135, 13479–13487

Table 3. Relevant Extinction Coefficients ε [mM^{-1} cm^{-1}] and EET Yields, η, from ZnMP to PCB (top) and PEB to ZnBC (bottom) in Various HP7-ApcEΔ Fusion Proteins[a]

EET parameters[b]		HP7::ApcEΔ	$ApcE\Delta_N$::HP7::$ApcE\Delta_C$	ApcEΔ::HP7
ZnMP → PCB	ε_D[c]	124	98.9	101
	ε_A[c]	3.79	3.67	3.05
	η[b]	32%	21%	30%
PEB → ZnBC	ε_D[d]	74.6	65.8	72.7
	ε_A[d]	18.5	13.9	16.7
	η[b]	50%	n.d.	33%

[a]The ZnMP→PCB system was excited at 415 nm, and the fluorescence emission determined at 675 nm. The PEB→ZnBC system was excited at 570 nm, and the fluorescence emission determined at 790 nm. [b]See Experimental Section for details of calculation. [c]415 nm. [d]570 nm.

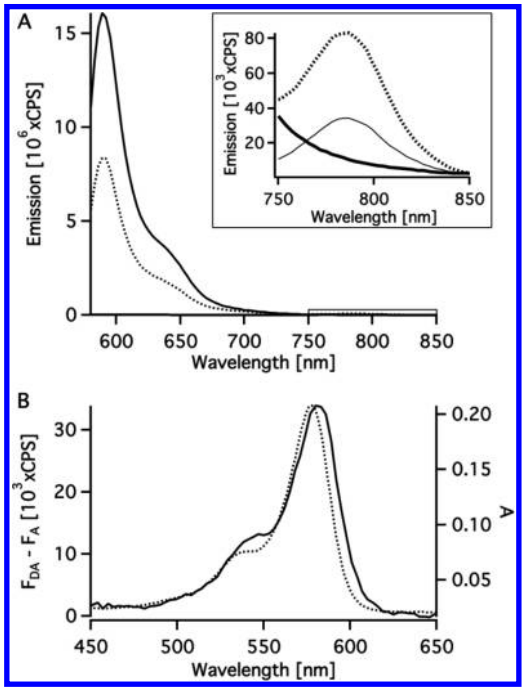

Figure 7. (A) Fluorescence emission spectra (λ_{ex} = 570 nm) of PEB-chromophorylated HP7::ApcEΔ with and without ZnBC (thick solid, and dotted lines, respectively). A rectangle marks the range shown in the inset where the weak emission from ZnBC is observed. The emission spectrum of the same concentration of ZnBC in non-chromophorylated HP7::ApcEΔ (thin solid line) is added for comparison. (B) Fluorescence excitation difference spectra (λ_{em} = 790 nm) of ZnBC bound to PEB-chromophorylated vs non-chromophorylated ApcEΔ::HP7 (solid line), overlaid on the respective absorption spectra of the PEB-chromophorylated protein (dotted line).

DISCUSSION

Directional EET through a network of pigments is the hallmark of photosynthetic light harvesting. It relies on specific proteins that assemble several types of pigments at well-defined spatial, energetic, and electronic configurations. This work aimed at constructing minimal functional representations of the elaborate light harvesting systems of cyanobacteria and red algae that integrate chlorophyll- and phycobilin-protein complexes, with a focus on the transfer step from the final donor of the PBS, L_{CM}, to the chlorophylls of the core antenna. To this end, we integrated the artificial heme- and Chl-binding protein, HP7, with ApcEΔ, a phycobilin-bearing water-soluble fragment of the natural phycobilisome core-membrane linker L_{CM}. Both proteins were chosen due to their simplicity and versatility: ApcEΔ comprises a single covalent phycobilin binding site that can be chromophorylated autocatalytically either with native PCB or with several other phycobilin derivatives; HP7 was originally designed as a heme-binding protein but was shown capable of binding other porphyrin and Chl derivatives. Unlike the covalently attached phycobilins, the porphyrin and Chl derivatives bind noncovalently but with high affinity to HP7. Both proteins are water-soluble but assemble as dimers in aqueous solutions. The pigment binding sites of HP7 are formed only upon its dimerization and assembly into a four-helix bundles form.

For generating the systems capable of binding both chromophore types, a HP7 domain lacking the cysteine responsible for covalent dimerization was fused to ApcEΔ at three different locations (Figure 1): preceding or following the N- or the C-terminus, respectively, and replacing the hydrophobic loop at positions 77−153 that was excised from the native ApcE in order to improve its solubility in water.[5] In all cases, fusing the HP7 motif did not interfere with, and in some cases even improved, the chromophorylation yields of the ApcE domain. The PCB absorption band was still red-shifted compared to phycocyanin in these constructs, but not as much as in native L_{CM}. The shifts of the phycobilin chromophore are independent of the presence or absence of the chlorophyll-type chromophore on the HP7 domain and, therefore, are the result of changes in the ApcE domain induced by the HP7 domain. The absorption spectra of PEB were not affected by the fusion of the HP7 domain. This indicates that the state of ring D contributes to the shifts observed with PCB, including the strong red-shift in ApcE, because this ring is no longer in conjugation in PEB.

The pigment binding capacity of the HP7 domain was retained in all fusion proteins. This implies the formation of four-helix bundles that can only occur if the hydrophobic surfaces of the two helices comprising HP7 remain accessible irrespective of the way they are fused. The formation of dimers and, in some cases, higher aggregates is also supported by size exclusion chromatography. Larger aggregates are, in particular, formed with the insertion construct, $ApcE\Delta_N$::HP7::$ApcE\Delta_C$, and its pigment complexes. In the N- or C-terminally fused constructs, the apparent aggregation numbers, N_{agg}, range from two to three, indicative of dimer or trimer formation. Notably, the apparent aggregation number of HP7::ApcEΔ heme complexes is 2.6 but the heme:protein stoichiometry is 1:1, which implies that all the HP7 domains form four-helix bundle dimers. Thus, it is reasonable to assume that, in the terminal fusion constructs, the increase in the apparent aggregation number reflects the formation of dimers with an extended nonglobular conformation rather than trimers. The aggregation numbers of the insertion construct, $ApcE\Delta_N$::HP7::$ApcE\Delta_C$, either as apoprotein or pigmented, are either six or close to nine, which is significantly higher than all the other respective proteins. Yet, the pigment binding stoichiometries to the HP7 domain are similar to the other variants. Following the same reasoning as above, an aggregation number of six would correspond to dimers of dimers, and an aggregation number of nine may reflect dimerization of the latter yielding octamers. Clearly, and not unexpectedly, placing the HP7 domain in the middle of the ApcE domain has the most pronounced effect on the protein structure, yet despite these structural variations the

binding capacities of both ApcE and HP7 are retained. Altogether, the spectroscopic and chromatographic data imply that, in the fusion proteins, neither the ApcEΔ nor the HP7 domains are grossly modified by each other. The most pronounced effect is the variation of the protein's aggregation state and overall shape. These variations are also reflected in the spectral shifts of PCB discussed above. However, the pigment binding capacity of the individual domain was maintained and, in the case of phycobilin binding, the yield of chromophorylation was even improved.

Aggregation of the water-soluble ApcE variants did not lead to significant EET between the phycobilin chromophores as indicated by their fluorescence anisotropy. This is in contrast to other phycobiliproteins, particularly allophycocyanin rod-core complexes. The latter are assembled from three heterodimeric ($\alpha\beta$) monomers into disc-shaped trimers whereby an α-PCB chromophore of one subunit is within 2.1 nm from a β-PCB chromophore of the neighboring subunit,[21] which leads to rapid subpicosecond EET between the chromophores.[22−28] The absence of intersubunit EET in the ApcE dimers suggests that the PCB and PEB chromophores are significantly further apart, and/or in unfavorable relative orientation for EET. An analysis of pairwise EET among the various PCB chromophores of phycocyanin trimers has shown that both factors can contribute dominantly, in addition to overlap integrals, to the efficiency of EET.[26]

The EET yields from ZnMP to PCB, and from PEB to ZnBC, were found to be around 30% for most of the ApcE-HP7 fusion proteins that were measured. The lowest yield, 21%, was measured for ZnMP to PCB in $ApcE\Delta_N$::HP7::$ApcE\Delta_C$, and the highest, 50%, for PEB to ZnBC in HP7::ApcEΔ. Applying a simple fluorescence resonance energy transfer (FRET) formalism, we evaluated the pigment distances within the different donor−acceptor systems. According to this formalism,[16] the EET yield, η, is given by

$$\eta = \frac{{R_0}^6}{{R_0}^6 + r}$$

where r is the distance between chromophores and R_0 is the Förster radius given by

$${R_0}^6 = 8.79 \times 10^{-5}[\kappa^2 n^{-4} \Phi_D \int_0^\infty F_D(\lambda)\varepsilon_A(\lambda)\lambda^4 \, d\lambda]$$

where κ^2 is an orientation factor, n is the refractive index of the solution, Φ_D is the fluorescence quantum yield of the donor, $F_D(\lambda)$ is the fluorescence spectrum of the donor, $\varepsilon_A(\lambda)$ is the molar absorption coefficient of the acceptor in units of M^{-1} cm^{-1}, λ is the wavelength in nm, and R_0 is in Å. Assuming n = 1.4 for an aqueous solution, κ^2 = 2/3 for unrestricted donor−acceptor relative orientations, and Φ_D values of 0.2 and 0.8 for ZnMP and PEB, respectively, the Förster radii of the ZnMP-PCB and PEB-ZnBC were estimated to be 51 Å and 58 Å, respectively. For an EET yield of 30%, these radii imply ZnMP-PCB and PEB-ZnBC distances of 59 Å and 67 Å, respectively. These distances seem long considering that both the ApcE and HP7 domains are small proteins, each spanning about 30 Å, which would imply that the chromophores in the constructs are as far apart as possible. However, assuming the relative orientation of the protein-bound donor and acceptor chromophores to be unrestricted is very unlikely, particularly in view of the highly anisotropic fluorescence of PEB and PCB. Variations and/or inaccuracies in fluorescence yields have only minor effects on the estimated distances because R_0 depends on the sixth root of Φ_D. Thus, smaller orientation factors, corresponding to perpendicular transition dipole moments of the donor and acceptor chromophores, and shorter distances are most likely to account for the observed EET yield. Additional structural information is required to determine the distances and relative orientations of the chromophores in the current donor−acceptor systems.

In conclusion, we have demonstrated the design and construction of small protein-pigment complexes analogous to natural light-harvesting systems of photosynthetic cyanobacteria. The protein scaffold was designed to have two distinct pigment binding domains: one for covalent binding of phycobilin chromophores and the other for noncovalent binding of porphyrin and Chl derivatives. The capability of each protein domain to bind different types of pigments has enabled the construction of versatile multipigment−protein complexes. Thus, we were able to assemble two bichromophoric systems that feature significant intramolecular EET. In one system, energy is transferred from the photoexcited porphyrin, ZnMP, to a phycobilin chromophore, PCB; and, in the other, a photoexcited phycobilin, PEB, transfers energy to a Chl derivative, ZnBC. This confirms that our modular, covalent approach for studying EET between the cyclic and open chain tetrapyrroles is reasonable and may be extended to larger structures mimicking light-harvesting in cyanobacteria. The design, construction, and characterization process demonstrated many of the advances in constructing such model systems, particularly in our ability to control the fold and aggregation state of protein-based systems. At the same time, it underlines the potential of exploiting the versatility and flexibility of protein-based systems in assembling multiple pigments into effective light-harvesting arrays and tuning the spectral properties of multichromophore systems.

EXPERIMENTAL SECTION

Fusion Protein Cloning and Expression. All genetic manipulations were carried out according to standard protocols.[10] The *hp7* gene (kindly provided by Prof. Ron Koder, City University of New York, New York, NY) was modified to replace the central cysteine (C32) by serine. The modified gene was combined with the plasmid pET-apcE(1−240/Δ77−153) carrying the modified *apcE*(1−240) gene of *Nostoc* sp. PCC7120 in which part of the putative loop domain (residues 77 to 153) was truncated.[3,5] Gene cloning, transformation, and expression generating PCB- and PEB-chromophorylated proteins were carried out as described by Tang et al.[5] but using potassium phosphate buffer (KPB) of pH 7.6 instead of pH 7.0 during the cell disruption step.

Purification of Chromophorylated Proteins. PCB- and PEB-chromophorylated proteins were separated from the apo-proteins by size-exclusion and anion-exchange chromatography, respectively, using an ÄKTA purifier liquid chromatography system (GE healthcare). PCB containing samples were dialyzed against KPB (20 mM, pH 6.5) containing NaCl (0.15 M), EDTA (5 mM), and urea (2 M), loaded onto a Sephacryl S-200HR preparative column (GE healthcare), and eluted at a flow rate of 1 mL/min with the same buffer. Fractions of 0.7 mL were collected, their UV−visible absorption spectra measured, and those with the highest ratio of PCB absorption at 660 nm to protein absorption at 280 nm were retained, pooled, and dialyzed against the same buffer without urea. Similarly, PEB samples were dialyzed against KPB (20 mM, pH 7.6) containing NaCl (0.05 M) and EDTA (2 mM), loaded onto a Hiprep DEAE FF 16/10 preparative column (GE healthcare), eluted at a flow rate of 1 mL/min with the same buffer and a linear 10 mM/min NaCl gradient, and collected in

0.7 mL fractions. Those featuring the highest ratio of PEB absorption at 576 nm to protein absorption at 280 nm were retained and pooled.

Determination of Protein Oligomerization States. Protein oligomerization states were determined by analytical size-exclusion chromatography using a 30 × 1.0 cm Superdex 200 column (GE healthcare). Ribonuclease A, carbonic anhydrase, ovalbumin, and α-globulin were used as standards for molecular weight calibration, and the column's void volume was determined with Blue Dextran 2000. A 0.2 mL sample of protein in KPB (20 mM, pH 7.4) containing NaCl (0.15 M) buffer was loaded on the column and eluted with the same buffer at a flow rate of 0.5 mL/min. Chromatograms were monitored simultaneously at 280 nm for protein absorption, and at pigment specific absorption wavelengths, namely, 369, 413, 415, 576, and 660 nm for ZnBC, heme, ZnMP, PEB, and PCB, respectively.

UV−vis-NIR Absorption and Fluorescence Spectroscopy. Absorption spectra were recorded in 1 cm cuvettes on a Jasco V-7200 spectrophotometer. Fluorescence excitation, emission, and anisotropy spectra were recorded in 3 × 3 mm cuvettes on a Fluorlog-3 spectrofluorometer (Horiba) equipped with Glan Thompson calcite prism automatic polarizers.

Phycobilin Binding Ratios. The phycobilin/protein ratios of PCB- and PEB-protein complexes were determined spectrophotometrically after denaturation with acidic urea (8 M, pH 1.5). The molar fractions of bound PCB, or PEB, in each protein were derived from Beer−Lambert law as follows, taking into account the chromophore absorption in the 280 nm range:

$$c_{\text{pigment}}/c_{\text{protein}} = \varepsilon_{\text{prot}}A_{\text{VIS}}/(\varepsilon_{\text{VIS}}A_{\text{UV}} - \varepsilon_{\text{UV}}A_{\text{VIS}})$$

where c_{pigment} and c_{protein} are the chromophore and protein concentration, respectively; A_{UV} and A_{VIS} are the absorbances at 280 nm and at the visible absorbance maximum of bound bilin (PCB or PEB, see below); ε_{UV} and ε_{vis} are the respective molar absorption coefficients; and $\varepsilon_{\text{prot}}$ is the protein's molar absorption coefficient at 280 nm. The latter was calculated from the amino acid sequence of each protein by using Sednterp (http://jphilo.mailway.com/download.htm). Values of 35 500 M^{-1} cm^{-1}[11] and 42 800 M^{-1} cm^{-1} were used for ε_{VIS} of PCB and PEB, respectively.[12] Using these values and the ratio $A_{\text{VIS}}/A_{\text{UV}}$ from absorption spectra of protein-free PCB and PEB, we derived values of 17 500 M^{-1} cm^{-1} and 13 800 M^{-1} cm^{-1} for the respective ε_{UV}. Once $c_{\text{pigment}}/c_{\text{protein}}$ was determined, it was possible to derive ε_{UV} and ε_{vis} for the protein-bound phycobilins from the absorption spectrum of the complex prior to denaturation.

Heme, ZnMP, and ZnBC Binding Stoichiometry. Typically, proteins at concentrations between 2 and 10 μM in 20 mM of pH 7.6 potassium phosphate buffer (KPB) containing 0.5 M NaCl were titrated with heme, ZnMP, or ZnBC. The concentrations of the proteins and pigments were determined spectroscopically. Protein extinction coefficients were calculated from the amino acid sequences. Pigment stock concentrations were determined by a four- to five-point calibration curve. Heme was dissolved in aqueous NaOH (10 mM) and calibrated in a 1:1 mixture of ethanol:50% acetic acid in water, using λ_{397} = 144 mM^{-1} cm^{-} at the pigment's peak absorption (397 nm).[13] ZnMP was dissolved and calibrated in DMSO, using ε_{575} = 17.7 mM^{-1} cm^{-1} at the pigment's peak absorption (575 nm).[14] ZnBC was dissolved in methanol and calibrated in KPB (20 mM, pH 7.6) containing NaCl (0.5 M), using ε_{760} = 39.0 mM^{-1} cm^{-1} at the pigment's peak absorption at 760 nm.[8,15]

Excitation Energy Transfer Yields. EET yields, η, were determined from enhanced acceptor emissions according to[16]

$$\eta = \left(\frac{\varepsilon_{\text{A}}(\lambda_{\text{D}}^{\text{ex}})}{\varepsilon_{\text{D}}(\lambda_{\text{D}}^{\text{ex}})}\right)\left(\frac{F_{\text{AD}}(\lambda_{\text{A}}^{\text{em}})}{F_{\text{A}}(\lambda_{\text{A}}^{\text{em}})}\right)\frac{1}{f_{\text{D}}}$$

where $F_{\text{AD}}(\lambda_{\text{A}}^{\text{em}})$ and $F_{\text{A}}(\lambda_{\text{A}}^{\text{em}})$ are the fluorescence emission of the acceptor in the presence and absence of a donor, respectively, detected at a wavelength corresponding to the acceptor emission, $\lambda_{\text{A}}^{\text{em}}$, and excited at the donor excitation wavelength, $\lambda_{\text{D}}^{\text{ex}}$; f_{D} is the fraction of occupied donor sites, and $\varepsilon_{\text{D}}(\lambda_{\text{D}}^{\text{ex}})$ and $\varepsilon_{\text{A}}(\lambda_{\text{D}}^{\text{ex}})$ are the molar absorption coefficients of donor and acceptor at $\lambda_{\text{D}}^{\text{ex}}$. In the ZnMP-PCB donor−acceptor system, it is possible to vary f_{D} gradually by titrating PCB-chromophorylated proteins with the ZnMP donor. Under conditions of strong binding, and prior to saturation $f_{\text{D}} = R_{\text{ZnMP}}$, where R_{ZnMP} is the molar ratio of ZnMP to protein. Substituting R_{ZnMP} for f_{D} above and rearranging gives

$$F_{\text{AD}}(\lambda_{\text{A}}^{\text{em}}) = F_{\text{A}}(\lambda_{\text{A}}^{\text{em}})\left(\frac{\varepsilon_{\text{D}}(\lambda_{\text{D}}^{\text{ex}})}{\varepsilon_{\text{A}}(\lambda_{\text{D}}^{\text{ex}})}\right)\eta R_{\text{ZnMP}} + F_{\text{A}}(\lambda_{\text{A}}^{\text{em}})$$

Since $F_{\text{A}}(\lambda_{\text{A}}^{\text{em}})$, the emission of the PCB-chromophorylated protein without ZnMP is constant, plotting $F_{\text{AD}}(\lambda_{\text{A}}^{\text{em}})$ as a function of R_{ZnMP} should yield a saturation binding curve, and η could be calculated from the slope and intercept of the linear region of the plot. Practically, we found the emission of PCB in the ApcE domain to be affected by up to 37% by the binding of ZnMP to the HP7 domain. To correct for this effect $F_{\text{A}}(\lambda_{\text{A}}^{\text{em}})$, and $F_{\text{AD}}(\lambda_{\text{A}}^{\text{em}})$ were normalized by the respective emission detected upon specific excitation of PCB at 660 nm.

In the PEB-ZnBC donor−acceptor system, it is only possible to titrate the ZnBC acceptor to a covalently bound PEB donor. In this case $F_{\text{A}}(\lambda_{\text{A}}^{\text{em}})$, and $F_{\text{AD}}(\lambda_{\text{A}}^{\text{em}})$ are the emissions of ZnBC bound to non-chromophorylated and PEB-chromophorylated protein, respectively, and f_{D} is unity.

■ ASSOCIATED CONTENT

Supporting Information

Table S1: Primers for minimization of apcE(1−240) and its fusion with hp7. Table S2: Plasmids used. Table S3: Absorption and fluorescence parameters of PCB- and PEB-chromophorylated ApcEΔ. Figure S1: Fluorescence excitation and anisotropy spectra of PCB- and PEB-chromophorylated ApcEΔ. Figure S2: Fluorescence emission spectra of ZnMP in PCB-chromophorylated and nonchromophorylated $\text{ApcE}\Delta_{\text{N}}$::HP7::$\text{ApcE}\Delta_{\text{C}}$, and ApcEΔ::HP7. Figure S3: Fluorescence excitation and anisotropy spectra (λ_{em} = 675 nm) of bichromophorylated ZnMP→PCB systems HP7::ApcEΔ, $\text{ApcE}\Delta_{\text{N}}$::HP7::$\text{ApcE}\Delta_{\text{C}}$, and ApcEΔ::HP7. This material is available free of charge via the Internet at http://pubs.acs.org.

■ AUTHOR INFORMATION

Corresponding Authors

*Tel/fax: +86-27-87284301, E-mail: khzhao@163.com.

#Tel: +972-4-6953511, Fax: +972-4-6944980, E-mail: drorn@migal.org.il.

Notes

The authors declare no competing financial interest.

■ ACKNOWLEDGMENTS

D.N. and K.H.Z. are grateful for support by the China-Israel Joint Research Program. K.H.Z. is grateful for support (21072068) from the National Natural Science Foundation of China, and support (2011PY075) from the Fundamental Research Funds for the Central Universities. D.N. is grateful for support by a personal research grant from the Israel Science Foundation.

■ ABBREVIATIONS

APC, allophycocyanin; ApcEΔ, ApcE(1−240/Δ77−153); EET, excitation energy transfer; PBS, phycobilisome; KPB, potassium phosphate buffer; PCB, phycocyanobilin; PcyA, PCB:ferredoxin oxidoreductase; PEB, phycoerythrobilin; PebS, PEB synthase; ZnBC, 13^2-OH-Zn(II)-bacteriochlorophyllide *a*; ZnMP, Zn(II) mesoporphyrin IX

■ REFERENCES

(1) Green, B.; Parson, W. *Light-harvesting antennas in photosynthesis*; Kluwer: Dordrecht, 2003.

(2) Gantt, B.; Grabowski, B.; Cunningham, F. X. In *Light-harvesting antennas in photosynthesis*; Green, B., Parson, W., Eds.; Kluwer: Dordrecht, 2003; pp 307−322.
(3) Zhao, K. H.; Su, P.; Böhm, S.; Song, B.; Zhou, M.; Bubenzer, C.; Scheer, H. *Biochim. Biophys. Acta, Bioenerg.* **2005**, *1706*, 81−87.
(4) Biswas, A.; Vasquez, Y. M.; Dragomani, T. M.; Kronfel, M. L.; Williams, S. R.; Alvey, R. M.; Bryant, D. A.; Schluchter, W. M. *Appl. Environ. Microbiol.* **2010**, *76*, 2729−2739.
(5) Tang, K.; Zeng, X.-L.; Yang, Y.; Wang, Z.-B.; Wu, X.-J.; Zhou, M.; Noy, D.; Scheer, H.; Zhao, K. H. *Biochim. Biophys. Acta, Bioenerg.* **2012**, *1817*, 1030−1036.
(6) Huang, S. S.; Koder, R. L.; Lewis, M.; Wand, A. J.; Dutton, P. L. *Proc. Natl. Acad. Sci. U. S. A.* **2004**, *101*, 5536−5541.
(7) Koder, R. L.; Valentine, K. G.; Cerda, J.; Noy, D.; Smith, K. M.; Wand, A. J.; Dutton, P. L. *J. Am. Chem. Soc.* **2006**, *128*, 14450−14451.
(8) Cohen-Ofri, I.; van Gastel, M.; Grzyb, J.; Brandis, A.; Pinkas, I.; Lubitz, W.; Noy, D. *J. Am. Chem. Soc.* **2011**, *133*, 9526−9535.
(9) Ajlani, G.; Vernotte, C. *Eur. J. Biochem.* **1998**, *257*, 154−159.
(10) Sambrook, J.; Fritsch, E.; Maniatis, T. *Molecular cloning: a laboratory manual.*, 2nd ed.; Cold Spring Harbour Laboratory Press: New York, 1989.
(11) Glazer, A. N.; Fang, S. *J. Biol. Chem.* **1973**, *248*, 659−662.
(12) Glazer, A. N.; Hixson, C. S. *J. Biol. Chem.* **1975**, *250*, 5487−5495.
(13) Weinstein, J. D.; Beale, S. I. *J. Biol. Chem.* **1983**, *258*, 6799−6807.
(14) Sakamoto, M.; Ueno, A.; Mihara, H. *Chem.—Eur. J.* **2001**, *7*, 2449−2458.
(15) Angerhofer, A.; Bornhauser, F.; Aust, V. V.; Hartwich, G.; Scheer, H. *Biochim. Biophys. Acta, Bioenerg.* **1998**, *1365*, 404−420.
(16) Lackowicz, J. R. *Principles of Fluorescence Spectroscopy*, 3rd ed.; Springer: New York, 2006; pp 443−475.
(17) Koder, R. L.; Anderson, J. L.; Solomon, L. A.; Reddy, K. S.; Moser, C. C.; Dutton, P. L. *Nature* **2009**, *458*, 305−309.
(18) Fry, H. C.; Lehmann, A.; Saven, J. G.; DeGrado, W. F.; Therien, M. J. *J. Am. Chem. Soc. 132*, 3997−4005.
(19) Tronin, A.; Strzalka, J.; Chen, X.; Dutton, P. L.; Ocko, B. M.; Blasie, J. K. *Langmuir* **2001**, *17*, 3061−3066.
(20) Zhang, J. M.; Zheng, X. G.; Zhang, J. P.; Zhao, F. L.; Xie, J.; Wang, H. Z.; Zhao, J. Q.; Jiang, L. J. *Photochem. Photobiol.* **1998**, *68*, 777−784.
(21) Brejc, K.; Ficner, R.; Huber, R.; Steinbacher, S. *J. Mol. Biol.* **1995**, *249*, 424−440.
(22) Debreczeny, M. P.; Sauer, K.; Zhou, J.; Bryant, D. A. *J. Phys. Chem.* **1995**, *99*, 8412−8419.
(23) Loos, D.; Cotlet, M.; De Schryver, F.; Habuchi, S.; Hofkens, J. *Biophys. J.* **2004**, *87*, 2598−2608.
(24) MacColl, R. *Biochim. Biophys. Acta, Bioenerg.* **2004**, *1657*, 73−81.
(25) Sharkov, A. V.; Kryukov, I. V.; Khoroshilov, E. V.; Kryukov, P. G.; Fischer, R.; Scheer, H.; Gillbro, T. *Biochim. Biophys. Acta, Bioenerg.* **1994**, *1188*, 349−356.
(26) Womick, J. M.; Miller, S. A.; Moran, A. M. *J. Chem. Phys.* **2010**, *133*, 024507.
(27) Womick, J. M.; Moran, A. M. *J. Phys. Chem. B* **2009**, *113*, 15747−15759.
(28) Womick, J. M.; Moran, A. M. *J. Phys. Chem. B* **2011**, *115*, 1347−1356.